

†Department of Pathology, Northwestern University Medical School, Chicago, Illinois 60611, USA

1. Hartwell, L. H., Hopfield, J. J., Leibler, S. & Murray, A. W. *Nature* **402**, 47–52 (1999).
2. Eisenberg, D., Marcotte, E. M., Xenarios, I. & Yeates, T. O. *Nature* **405**, 823–826 (2000).
3. Uetz, P. et al. *Nature* **403**, 623–627 (2000).
4. Xenarios, I. et al. *Nucleic Acids Res.* **28**, 289–291 (2000).
5. Jeong, H., Tombor, B., Albert, R., Oltvai, Z. N. & Barabási, A.-L. *Nature* **407**, 651–654 (2000).
6. Amaral, L. A., Scala, A., Barthelemy, M. & Stanley, H. E. *Proc. Natl Acad. Sci. USA* **97**, 11149–11152 (2000).

7. Rain, J.-C. et al. *Nature* **409**, 211–215 (2001).
8. Albert, R., Jeong, H. & Barabási, A.-L. *Nature* **406**, 378–382 (2000).
9. Winzler, E. A. et al. *Science* **285**, 901–906 (1999).
10. Ross-Macdonald, P. et al. *Nature* **402**, 413–418 (1999).
11. Fell, D. A. & Wagner, A. in *Animating the Cellular Map* (eds Hofmeyr, J.-H., Rohwer, J. M. & Snoep, J. L.) 79–85 (Stellenbosch Univ. Press, 2000).
12. Wagner, A. *Nature Genet.* **24**, 355–361 (2000).
13. Costanzo, M. C. et al. *Nucleic Acids Res.* **28**, 73–76 (2000).

Cell culture

Progenitor cells from human brain after death

Culturing neural progenitor cells from the adult rodent brain has become routine^{1,2} and is also possible from human fetal tissue^{3,4}, but expansion of these cells from postnatal and adult human tissue, although preferred for ethical reasons, has encountered problems^{5–8}. Here we describe the isolation and successful propagation of neural progenitor cells from human post-mortem tissues and surgical specimens. Although the relative therapeutic merits of adult and fetal progenitor cells still need to be assessed, our results may extend the application of these progenitor cells in the treatment of neurodegenerative diseases.

As a source of neural progenitor cells, we used brain tissue from an 11-week-old post-natal male, who died of extracerebral complications of myofibromatosis, and from a resected temporal cortex from a 27-year-old male (courtesy of J. Alksney). The tissue was removed, sectioned 2 hours after death and placed in cold antibiotic-containing Hank's buffered-salt solution, then processed for culture 3 hours later. Representative sections of hippocampus, ventricular zone, motor cortex and corpus callosum were taken. The temporal cortex tissue was provided *en bloc* and placed in chilled Hank's buffered-salt solution and processed for culture 3 hours after removal. The adult tissues were divided into hippocampal formation, white matter and remaining cortical grey matter. Tissues were finely diced and then dissociated by enzymic digestion with papain, DNase I and neutral protease for 45 min at 37 °C, as described for rodent tissue¹.

We initially plated isolated cells onto fibronectin-coated plates in DMEM:F12 medium containing glutamine, amphotericin-B, penicillin, streptomycin and 10% fetal bovine serum. After 24 hours, the medium was replaced with DMEM:F12 supplemented with BIT-9500 (bovine serum albumin, transferrin, insulin; Stem Cell Technologies), 20 ng ml⁻¹ basic fibroblast growth factor (FGF-2), 20 ng ml⁻¹ epidermal growth factor, and 20 ng ml⁻¹ platelet-derived growth factor AB.

We had limited success using these condi-

tions, but when the medium was supplemented with 25% conditioned medium from rat stem cells that had been genetically modified to overproduce a secreted form of FGF-2 and its stem-cell cofactor, the glycosylated form of cystatin C (ref. 9), plating efficiency, as well as initial survival and growth, greatly improved. The medium was changed every two days and the cultures were replated onto twice the surface area to accommodate proliferative expansion. All tissue samples gave neural progenitor cells, but the highest yields were from hippocampus and ventricular zone. For long-term storage, cultures were

dissociated with trypsin, rinsed and cryopreserved in growth medium (without growth factors) containing 10% dimethylsulphoxide.

Cells from the 11-week-old tissue grew at log phase for more than 70 population doublings before showing signs of *in vitro* senescence (a significant reduction in growth rate). The adult tissues were expanded for more than 30 doublings before senescence (Fig. 1). Neurons were spontaneously generated at all stages in these cultures (Fig. 1a,b), and more complete differentiation could be induced by withdrawing growth factors and stimulating the cells with forskolin and retinoic acid (Fig. 1c)^{1,9}. Neonatal and adult cultures produced similar proportions of neurons and astrocytes, although the number of spontaneously generated neurons was lower than reported for fetal cultures^{3,4} and decreased significantly as cultures reached senescence. Oligodendrocytes were rare in most cultures.

So far, we have processed 23 tissue samples from people of different age groups. Most samples have yielded viable progenitor cells, with the longest post-mortem interval

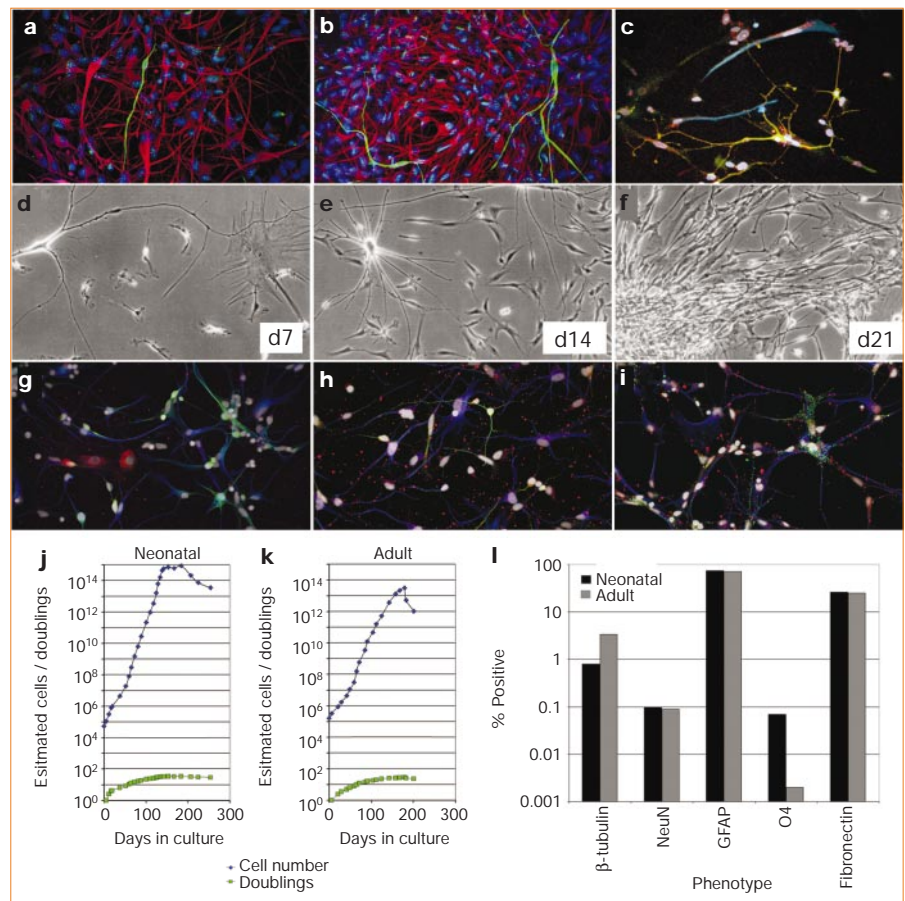


Figure 1 Neural progenitor cells isolated from postmortem human brain. **a–i**, Cells obtained from brains of two males: an 11-week-old neonate (**a–c**) and a 27-year-old adult (**d–i**). Proliferative cells (**a, b**) were stained¹ for immature neurons (β -tubulin; green), astrocytes (GFAP; glial fibrillary acidic protein; red) and nuclei (DAPI stain; blue). Differentiated cells (**c**) were stained for neurons: Map2abc (red) and neurofilament 150 (green), for GFAP (blue), and nuclei (white). Adult cells as seen by phase-contrast microscopy at days (d) 7, 14 and 21 after plating (**d–f**). Differentiated cells are shown in the third row: **g**, fibronectin (fibroblasts, red), β -tubulin (green), GFAP (blue), nuclei (white); **h**, Map2abc (green), GFAP (blue), nuclei (white); **i**, immature glia (A2B5, green), GFAP (blue), nuclei (white). The growth of neonatal and adult cells in culture is shown in the bottom row: **j, k**, phenotypic counts of differentiated neonatal and adult cells, respectively; **l**, immunostaining of differentiated cells: NeuN, post-mitotic neuron marker; O4, immature oligodendrocyte marker; fibronectin, connective tissue.

before culture being about 20 hours. Tissues from young individuals yield significantly more cells per gram and these cells have a higher proliferative capacity. Intrinsic differences in growth potential and/or lineage potential may affect the utility of cell transplantation or other applications for therapy. Questions relating to the *in vitro* lifespan of these cells and the role of telomerase¹⁰, as well as the importance of DNA methylation, still need to be addressed.

Using cells cultured from embryonic tissues bypasses some of these concerns, but also raises complex ethical and societal issues. Careful evaluation and consideration of the relative merits of post-mortem or adult-derived cells and fetal progenitor cells will be necessary.

Theo D. Palmer*†, Philip H. Schwartz‡, Philippe Taupin*, Brian Kaspar*, Stuart A. Stein‡, Fred H. Gage*

*The Salk Institute, Laboratory of Genetics, 10010 North Torrey Pines Road, La Jolla, California 92122, USA

e-mail: gage@salk.edu

†Stanford University, Department of Neurosurgery, MSLS P304, 1201 Welch Road, Stanford, California 94305-5487, USA

‡Children's Hospital of Orange County, Brain and Tissue Bank for Developmental Disorders, 455 South Main Street, Orange, California 92868, USA

- Palmer, T. D., Markakis, E. A., Willhoite, A. R., Safar, F. & Gage, F. H. *J. Neurosci.* **19**, 8487–8497 (1999).
- Reynolds, B. A. & Weiss, S. *Science* **255**, 1707–1710 (1992).
- Svendsen, C. N., Caldwell, M. A. & Ostendorf, T. *Brain Pathol.* **9**, 499–513 (1999).
- Fricker, R. A. *et al. J. Neurosci.* **19**, 5990–6005 (1999).
- Pincus, D. W. *et al. Ann. Neurol.* **43**, 576–585 (1998).
- Johansson, C. B., Svensson, M., Wallstedt, L., Janson, A. M. & Frisen, J. *Exp. Cell Res.* **253**, 733–736 (1999).
- Pagano, S. F. *et al. Stem Cells* **18**, 295–300 (2000).
- Roy, N. S. *et al. Nature Med.* **6**, 271–277 (2000).
- Taupin, P. *et al. Neuron* **28**, 385–397 (2000).
- Ostendorf, T. *et al. Exp. Neurol.* **164**, 215–226 (2000).

Boundary effects

Refraction of a particle beam

The refraction of light at an interface is familiar as a rainbow or the ‘bending’ of a pencil in a glass of water. Here we show that particles can also be refracted and even totally internally reflected, as evidenced by an electron beam of 28.5×10^9 electron volts being deflected by more than a milliradian upon exiting a passive boundary between a plasma and a gas — the electron beam is bent away from the normal to the interface, just like light leaving a medium of higher refractive index. This phenomenon could lead to the replacement of magnetic kickers by fast optical kickers in particle accelerators, for example, or to compact magnet-less storage rings in which beams are guided by plasma fibre optics.

Refraction is caused by electrostatic plasma fields set up when plasma electrons are

expelled by the collective space charge force of the head of the beam. The plasma ions in the beam path are more massive and remain, constituting a positively charged channel through which the latter part of the beam travels. The ions provide a net force that focuses the beam^{1,2}. When the beam comes close to the plasma boundary, the ion channel becomes asymmetric, producing a deflecting force in addition to the focusing force. This formation of an asymmetric plasma lens³ gives rise to the bending of the beam path at the interface.

The order of magnitude of this deflection can be estimated, yielding an expression for the deflection angle, Θ , as a function of the incident angle, ϕ . This is the effective non-linear Snell's law for the electron beam refraction, valid for ϕ greater than Θ :

$$\Theta = (8 \alpha N r_e) / (\pi \sqrt{2\pi} \gamma \sigma_z \sin \phi)$$

where $N/\sqrt{2\pi}\sigma_z$ is the charge per unit length of the beam, r_e is the classical electron radius, γ is the beam's energy in units of mc^2 and α is a factor of order one that is a weak function of plasma density and bunch length. When ϕ is less than Θ , this equation breaks down and the beam is internally reflected. Simulations⁴ show that $\Theta \approx \phi$ (critical reflection) for small values of ϕ .

We tested this analytical model by using the electron beam at the Stanford Linear Accelerator Center (Final Focus test facility), as described^{5,6}. Sample results are shown in Fig. 1 and compared with a full three-dimensional electromagnetic particle-in-cell computer simulation⁷. In Fig. 1a, the solid curve represents the prediction from the model (with $\alpha = 0.2$): for incident angles smaller than 1.3 mrad, the beam appears to be internally reflected, in agreement with the model.

Figure 1b shows a snapshot of the real

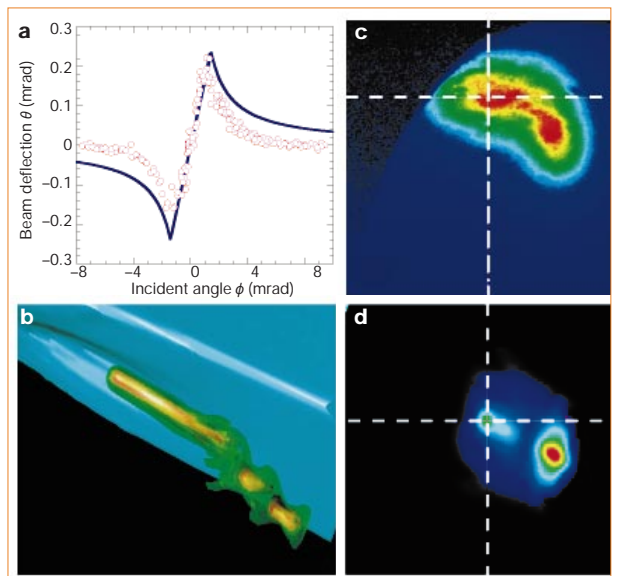


Figure 1 Experimental and simulation results demonstrating refraction of an electron beam at a plasma-gas interface. **a**, Actual electron-beam deflection (circles), measured using a beam-position monitor, and the theoretical deflection (blue line) as a function of the incident angle. **b**, Simulation: perspective image of a beam emerging from plasma (turquoise); the inward motion of the plasma electrons is visible as a depression in the plasma surface behind the beam. **c**, Experiment: image of the beam downstream of the plasma, showing the deflected beam and the undeflected transient (at the crosshairs); **d**, head-on view of image in **b**. The beam consisted of 1.9×10^{10} electrons at 28.5 GeV in a gaussian bunch of length $\sigma_z = 0.7$ mm and spot size $\sigma_x \approx \sigma_y \approx 40$ μm . The plasma, with radius 2.3 mm, length 1.4 m and density 1×10^{14} cm^{-3} , was created by photoionization of lithium vapour by an ArF laser. The angle, ϕ , between the electrons' initial trajectory and the plasma boundary was controlled by adjusting the tilt angle of the final laser-beam mirror.

space of the beam and plasma electron density (turquoise) from a simulation. A transient at the head of the beam is apparent because of the finite time that it takes the plasma to respond to the beam. The tail portion is deflected towards the plasma and is near the plasma boundary. The transient results in the characteristic splitting of the beam images downstream, as shown in Fig. 1c, d.

The simulations and experimental results presented here show that it is possible to refract and even reflect a particle beam from a dilute plasma gas. Remarkably, for a 28.5-GeV beam that can bore through several millimetres of steel, the collective effects of a plasma are strong enough to ‘bounce’ the beam off an interface that is one million times less dense than air.

Patric Muggli*, Seung Lee*, Thomas Katsouleas*, Ralph Assmann†, Franz-Joseph Decker†, Mark J. Hogan†, Richard Iverson†, Pantaleo Raimondi†, Robert H. Siemann†, Dieter Walz†, Brent Blue‡, Christopher E. Clayton‡, Evan Dodd‡, Ricardo A. Fonseca‡, Roy Hemker‡, Chandrashekar Joshi‡, Kenneth A. Marsh‡, Warren B. Mori‡, Shoquin Wang‡

*University of Southern California, Los Angeles, California 90089, USA

e-mail: katsoule@usc.edu

†Stanford Linear Accelerator Center, Stanford University, Stanford, California 94309, USA

‡University of California, Los Angeles, California 90095, USA

- Su, J. J., Katsouleas, T. & Dawson, J. M. *Phys. Rev. A* **41**, 3321–3331 (1990).
- Whittum, D., Sessler, A. & Dawson, J. M. *Phys. Rev. Lett.* **64**, 2511–2514 (1990).
- Chen, P. *Part. Accel.* **20**, 171–182 (1987).
- Katsouleas, T. *et al. Nucl. Instrum. Meth. Phys. Res. A* **455**, 161–165 (2000).
- Muggli, P. *et al. Phys. Rev. Sp. Top. AB* (submitted).
- Hogan, M. J. *et al. Phys. Plasmas* **7**, 2241–2248 (2000).
- Hemker, R., Mori, W. B., Lee, S. & Katsouleas, T. *Phys. Rev. Sp. Top. AB* **3**, 61301–61305 (2000).